

# Polymer nanotubes and nanowires for integrated photonics

N. Huby, J. Bigeon, B. Bêche  
Institut de Physique de Rennes UMR  
CNRS 6251,  
263 avenue Général Leclerc  
Rennes, France

J.-L. Duval  
Institut des Matériaux,  
UMR CNRS 6502  
2 rue de la Houssinière  
Nantes, France

D. Duval  
Nanobiosensors and Bioanalytical  
Applications Group  
CIN2 (CSIC) and CIBER-BBN  
Campus UAB, Barcelona, Spain

**Organic 1D-nanostructures are elaborated and characterized for applications in integrated photonics. The wetting template method enables the control of aspect ratio (length and diameter) of hollow or filled individual 1D-nanostructure. Organic nanotubes and nanowires are integrated on photonic chips. An optical coupling occurs with integrated organic micro-structures (disk-reservoir) and allows propagation in 1D-nanostructures with losses about hundred db/mm. Nanotubes are here particularly interesting since they are easy to produce and they present a lack of investigation in nanophotonics.**

*keywords-nanotubes, polymer, interconnections, integrated optical circuit, wetting template, UV-lithography*

## I. INTRODUCTION

Integrated photonics offers great opportunities for components and devices with increasing requirements in terms of higher performances, wider applicability, lower energy consumption, high speed data transport and highly sensitive sensors. The comprehension of optical properties at the nanometer scale and the design of densely packed photonic devices are two essential fields of investigation. High aspect ratio nanostructures (nanowires and nanotubes) are particularly attractive for controlling and modulating light. Sub-wavelength structures are based on spatial optical confinement at nanoscale which modifies light propagation and light-matter interaction. This near field feature can interlink and process optical signals more efficiently, which makes it very attractive for on-chip data transport. The second major application directly concerned is related to highly sensitive sensors. Within the evanescent field, small changes at, or near, the surface can be probed. This makes 1D-nanostructures based devices much more sensitive than other evanescent-based sensors fabricated by planar lithography technique.

A large number of studies have been reported on dielectric nanowires based photonic devices (inorganic and organic) while nanotubes (other than carbon nanotubes) present a real lack of investigation for photonics applications. Due to the technological rupture in material processes, organic 1D-nanostructures emerged as a new class of building blocks in nanophotonics [1,2,3,4]. Indeed strategies based on organic materials (small molecules and polymers) are of great interest since they are flexible, biocompatible,

multifunctional, energy friendly and cheap. Behind these advantages the main attractive aspect is their liquid-phase processability enabling innovative fabrication methods.

## II. FABRICATION OF 1D-NANOSTRUCTURES

The nanotubes and nanowires fabrication has been performed by the wetting template strategy [5] described in Figure 1. Commercially available 60- $\mu\text{m}$  thick alumina porous membranes (anodized aluminium oxide, AAO) are impregnated with SU8 photoresist. This chemically amplified polymer is sensitive to near UV radiation, presents thermal stability and is available in a wide range of formulations covering a large variety of viscosities. Two resins have been used in this work: the SU8-2002 and the SU8-2025 with viscosity of 2.49 Pa.s and 4500 Pa.s respectively. First, the AAO membrane is placed onto a resist film at room temperature (Figure 1a). For the most viscous SU8, the temperature is then increased up to 60°C in order to lower the viscosity and so to favour the impregnation. After diffusion of the SU8 in the 200 nm-diameter pores of the membrane, the whole sample was exposed to UV light ( $\lambda=365$  nm) for polymerisation (Figure 1b).

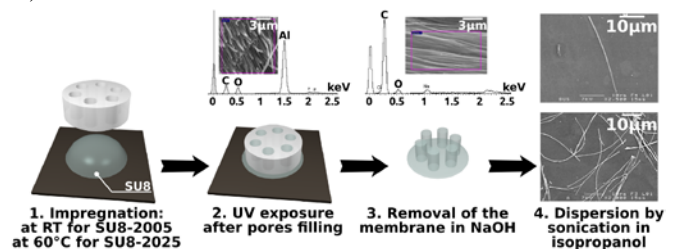


Figure 1: Wetting template method for 1D-nanostructures elaboration. The filled or hollow aspect is related to the viscosity of the SU8 photoresist.

After the full conversion of the resin (200 mJ/cm<sup>2</sup>), the sample is immersed in a selective NaOH (1.5 M) solution for 12 hours leading to the full dissolution of the membrane (Figure 1c). The solution was centrifuged in order to replace NaOH with isopropanol. EDS (energy dispersive X-ray spectroscopy) measurements have been performed before and after the NaOH treatment in order to control the efficient removal of the membrane. Finally, the dispersion of nanotubes or nanowires into isopropanol (chosen for its

low surface tension  $\gamma=21.8$  N/m) is improved by a ultrasonication (Figure 1d).

The resulting nano-objects exhibit different morphology according to the resist viscosity. The more viscous polymer SU8-2025 leads to nanowires while the less viscous one SU8-2002 forms tubular objects. The reason is related to impregnation mechanism. Indeed the diffusion into the whole thickness of the membrane is significantly faster for the less viscous resin (few minutes compared with half an hour for the more viscous).

### III. THEORETICAL WAVEGUIDING BEHAVIOUR

Theoretical study of the modal waveguiding behaviour in such nanostructures is presented. The eigenvalue equation deduced from Maxwell's equations has been solved by implementing it in Matlab software. Regarding the nanowire geometry, propagation characteristics are obtained by solving the well-known eigenvalues equations of the single clad fiber. The effective index  $n_{eff}$  for each of the four first modes is plotted as a function of the NW diameter  $\phi$  normalized by the wavelength  $\lambda$  in Figure 2a. The grey zone is related to the NWs fabricated in this work. As the only existing mode is  $HE_{11}$ , single mode propagation is anticipated.

The theoretical investigation of optical propagation in nanotubes geometry is based on an analytical formalism developed recently [6]. The modal cut-off thicknesses of the NTs are obtained by resolving numerically the eigenvalue equations. These cut-off values (outer  $\phi_{out}$  and inner  $\phi_{in}$  diameter) govern the presence or not of a mode in the structure. An exception arrives for the hybrid mode  $HE_{11}$  which is always present in cylinder structures.

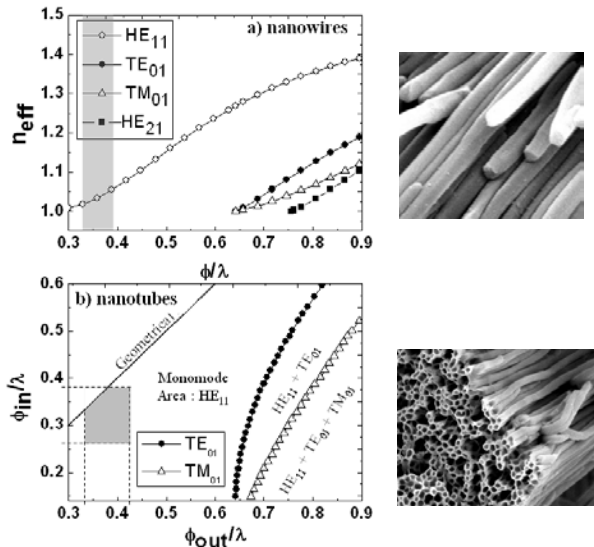


Figure 2 Theoretical investigations. a) Effective refractive index  $n_{eff}$  versus the normalized diameter of the NWs. b) Map of mode areas for SU8 nanotubes as a function of inner  $\phi_{in}$  and outer  $\phi_{out}$  diameters. The grey zones highlight the area related to the nanostructures fabricated here.

Cut-off values are plotted for the  $TE_{01}$  (transverse electric) and  $TM_{01}$  (transverse magnetic) modes as the normalized inner diameter  $\phi_{in}/\lambda$  versus normalized outer diameter  $\phi_{out}/\lambda$ .

As a result a map of monomode and multimode areas for tubular structures is depicted in Figure 2b. The geometrical limit corresponds to the fact that  $\phi_{in}$  cannot exceed  $\phi_{out}$ . The grey zone highlights the area related to NTs fabricated as described afterward. It clearly proves that only a single mode feature exists in these SU8 nanotubes.

### IV. INTEGRATION ON PHOTONIC CHIP

SU8 NTs and NWs have been integrated along organic SU8 microstructures designed on a photonic chip in order to evaluate their optical waveguiding properties. The SU8 microstructures were previously patterned on a Si/SiO<sub>2</sub> substrate by a one-step UV-lithography process. The chip consists of microstructures such as ridge waveguides (6  $\mu$ m width) and photons disk-reservoirs (200  $\mu$ m-radius disk) where the light is confined at the edges of the curved structures. These disk-reservoirs are particularly interesting for coupling with sub-wavelength object since the evanescent tail is displaced in the low-index medium (air) due to the curvature radius.

Top-view field intensity map have been recorded during light propagation in single nanostructure. The strong confinement of the field in a coupling zone between a disk-reservoir and a single NT or a single NW is shown on Figure 4a and 4b respectively. In both cases, the light is confined at the edge of the disk and throughout the NT and NW. Experimental data analysis leads to scattering losses about hundred dB/mm [7] for red and infrared light.

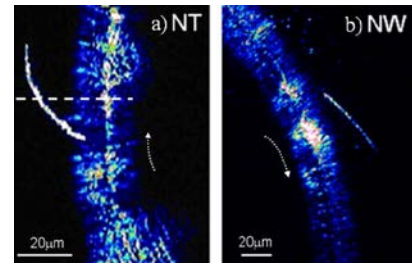


Figure 4: Schematic illustration of the photonic chip Light is injected into the core of the waveguide on the right side and propagates to the disk reservoir where whispering gallery modes (WGM) are excited.

### ACKNOWLEDGMENTS

The authors thank A. Carré, Cyril Hamel and Ludovic Frein for technical support as well as J. Le Lannic for SEM images. These works were supported by Region Bretagne and Pays de la Loire.

### REFERENCES

- [1] W. T. Hammond, and J. Xue, Appl. Phys. Lett. **97**, 073302 (2010)
- [2] Xing X.; Zhu H., Wang Y.; Li B. *Nanolett.* **2008**, 8, 2839.
- [3] J. J. Ju, S. K. Park, S. Park, J. Kim, M.-S. Kim, M.-H. Lee, and J. Y. Do, Appl. Phys. Lett. **88**, 241106 (2006).
- [4] O'Carroll D.; Lieberwirth L.; Redmond G. *Nat. Nanotech.* **2007**, 2, 180.
- [5] Steinhart M.; Wendorff J.H.; Greiner A.; Wehrspohn R.B.; Nielsch K.; Schilling J.; Choi J.; Gösele U. *Science* **2002**, 296, 1997.
- [6] Duval D.; Bêche B. *J. Opt.* **2010**, 12, 075501.
- [7] N. Huby, J.-L. Duvail, D. Duval, D. Pluchon and B. Bêche' Appl. Phys. Lett. **99**, 113302 (2011)